Packet Drop Probability Analysis of Dual Energy Harvesting Links With Retransmission

Mohit K. Sharma and Chandra R. Murthy, *Senior Member, IEEE*

***Abstract*— In this paper, we consider point-to-point *dual* energy harvesting (EH) links, where both transmitter and receiver are EH nodes (EHNs), with a retransmission protocol: either an automatic repeat request (ARQ) or hybrid ARQ with chase combining. We develop a framework to analyze the impact of various physical layer parameters, e.g., *the energy harvesting profiles, size of energy buffer, and power management policies*, at both the transmitter and receiver, and the *channel statistics and coherence time*, on the packet drop probability (PDP) of dual EH links over block fading channels. We derive the *closed-form* expressions for the PDP of a retransmission index-based power management policy. The presented framework naturally extends to obtain the PDP of *mono* EH links, i.e., links where only one of the two nodes harvests energy. To obtain further insights, we analyze the PDP of links with *zero* and *infinite* energy buffer size, and characterize the *energy unconstrained regime*, where the PDP is governed only by the average harvesting rate. Through extensive Monte Carlo simulations, we demonstrate the accuracy of the theoretical expressions, compare performance against existing power management schemes, and illustrate the performance tradeoffs involved.**

***Index Terms*— Energy harvesting, ARQ, HARQ-CC, packet drop probability, Markov chain.**

I. Introduction

MANY intended applications of energy harvesting (EH) wireless sensor networks (WSNs) [2], such as surveillance, structural monitoring, etc. require highly reliable links, in order to collect timely and meaningful information [3]. Since an EH node (EHN) garners energy from the environment, the randomness in the EH process, along with the finiteness of the energy storage buffers, pose novel challenges for the design of reliable EH links. The retransmission protocols, coupled with transmit power control, are a popular choice for enhancing the reliability, and are already part of low power communication standards such as IEEE 802.15.4 [4]. For retransmissions with fixed size packets, the packet drop probability (PDP) is used as a metric of reliability [5], [6]. In EH based WSN applications involving distributed processing and data relaying, it is important to analyze the PDP of dual EH links, i.e., the links whose both transmitter and receiver are EHNs.

In this work, we consider an EH based monitoring application, where periodic measurements are taken by a transmitting EHN, and are useful only if they are delivered by a deadline to a receiving EHN. Provided there is enough energy available at both the EHNs, a packet containing the measured data can be transmitted at most K times. After each attempt, the transmitter receives an acknowledgment (ACK) if the packet is successfully delivered, or else it receives a negative ACK (NACK). If the packet is not successfully delivered by the deadline, it is *dropped*. The PDP is defined as the average fraction of packets that are dropped.

The aim of this paper is to develop a general framework to understand the impact of various physical layer parameters on the PDP of dual EH links. For example, the PDP is a function not only of the transmit power levels at which the different attempts are made, but also of other parameters, namely, the EH profiles, and sizes of the energy buffers at the EHNs, the channel statistics and coherence time. The dependence of PDP on these parameters is not clear, and its systematic study can lead to insights about the joint impact of system parameters on the PDP. The design of PDP optimal policies based on the analytical expressions derived in this paper is considered in our follow up work [7].

Considering an EH receiver makes it pertinent to study the impact of data processing at the receiver. To this end, in addition to the automatic-repeat-request (ARQ) protocol, we also consider hybrid ARQ with chase combining (HARQ-CC). In HARQ-CC, a NACK results in a retransmission, but unlike the ARQ, the receiver in HARQ-CC attempts to decode the packet by maximal ratio combining (MRC) all the copies of the packet received in previous attempts. In conventional communication systems, HARQ-CC offers an improvement in the PDP over the ARQ protocol. However, the results obtained in this paper show that the performance gain obtained for systems with an EH receiver may be relatively insignificant, when either the transmitter or receiver is highly energy-starved (see Fig. 5). Our results analytically characterize the PDP of both ARQ and HARQ-CC as a function of physical layer parameters. In the next subsection, we present a brief summary of related work.

A. Related Work

In recent years, the performance of point-to-point *mono* EH wireless links, i.e., links with an EH transmitter and a conventional receiver, herein referred to as *mono-T* links, has been studied under various design objectives, e.g., information-theoretic capacity [8]–[10], event loss probability [11], delay [12], throughput [13]–[15], and PDP [16]–[18]. The throughput of mono EH links where only the receiver is EHN, called as *mono-R*, is maximized in [19] and [20].

Manuscript received January 7, 2016; revised May 14, 2016; accepted August 8, 2016. Date of publication September 20, 2016; date of current version December 29, 2016. This work was supported by the Research Grant from the Aerospace Network Research Consortium. This paper was presented at IEEE Global Conference on Signal and Information Processing, December 2014 [1].

The authors are with the Indian Institute of Science, Bangalore 560012, India (e-mail: mohit@ece.iisc.ernet.in; cmurthy@ece.iisc.ernet.in).

Color versions of one or more of the figures in this paper are available online at http://ieeexplore.ieee.org.

Digital Object Identifier 10.1109/JSAC.2016.2611919

An excellent overview of recent results in the area can be found in [21].

Determining the fundamental performance limits (i.e., the capacity) of dual EH links with finite energy buffers is still an open problem. Arafa and Ulukus [22] maximize the throughput of a dual EH link, and characterize the so-called maximum departure region for a MAC. However, the analysis ignores the effect of fading and the time varying nature of the wireless channel, and does not consider the retransmissions. The delay limited throughput of ARQ based dual EH link for fast fading channels, and with a fixed-power policy is analyzed in [23]. However, the PDP of dual and mono-R links, as well as of HARQ-CC based mono-T links has not been analyzed.

Medepally *et al.* [16] analyze the PDP of ARQ based mono-T EH links for both slow and fast fading channels, when a fixed (constant) power is used for all attempts. Aprem *et al.* [17] generalized the analysis of [16], for policies where the transmit power is an affine function of the attempt index. The PDP expressions obtained in [16] and [17] are recursive in nature. On the other hand, Devraj *et al.* [18] design PDP optimal policies for ARQ-based mono-T EH links with infinite size battery. This analysis does not require closed-form expressions for the PDP. However, the PDP analysis of dual EH links requires one to consider the interaction between the EH processes at both nodes, which makes it fundamentally different from the analysis of mono EH links in [16] and [17].

Recently, there has been a growing interest in designing policies which mitigate the imperfections of the battery, such as battery degradation [24] and lack of accurate state-of-charge (SoC) information [25]–[27]. Michelusi *et al.* [27] show that with sufficiently large battery, the optimal throughput can be achieved with only 1-bit SoC knowledge, provided the throughput is a linear function of the transmit power. Srivastava and Koksal [28] present near-optimal policies, which operate with only 1-bit SoC knowledge. Moreover, the knowledge of the EH process can be used as a substitute for SoC information [26]. These considerations have lead to the concept of SoC-unaware policies which operate independent of SoC information, e.g., fixed power policies [16], and generalized linear power policies [17], [23]. However, the performance of such policies has not been studied systematically and needs to be benchmarked. In this work, we analyze the PDP of *retransmission index-based* policies (RIPs), which provide an attempt-based prescription of transmit power, and benchmark it against the optimal policies.

B. Contributions

Our main contributions in this paper are as follows:

1) We present a rigorous analysis of the PDP of dual EH links, for both ARQ and HARQ-CC. We obtain recursive, exact expressions for the PDP by modeling the system evolution as a discrete-time Markov chain (Sec. III).
2) Using the insight that the conditional PDP only depends on the number of feasible attempts in a frame, and not on the precise energy arrival and departure instants, we derive *closed-form* expressions for the PDP of dual EH links. We show that the number of feasible attempts can be exactly determined when: (i) the batteries at the transmitter and receiver are large enough to store the energy required to support all the attempts in a frame, and (ii) the energy used for each attempt exceeds the energy harvested in a single slot. In these cases, the closed-form PDP expressions are exact. In other cases, the closed-form expression provides an upper bound on the actual PDP. We demonstrate the accuracy of the closed-form expressions in a wide range of scenarios through simulations (Sec. IV).
3) We also analyze the PDP for the links with zero and infinite batteries. In the latter case, we characterize the so-called energy unconstrained regime (EUR) of mono and dual EH links (Sec. V).
4) We show that our framework extends naturally to obtain the PDP of mono EH links (Sec. VI) and also to spatially and temporally correlated EH processes (Sec. VII).

The PDP analysis presented in this paper generalizes that in [16] and [17] by considering the EH receiver, spatio-temporal correlation of EH processes at both the EHNs, and the impact of data processing at the receiver. Moreover, the framework developed here is very general, and can be easily extended to other retransmission based protocols such as HARQ with incremental redundancy [29]. The obtained results provide useful insights, e.g., the HARQ-CC improves the PDP (by a factor of 10), compared to ARQ, provided the receiver harvests sufficient energy to support the extra signal processing required. In contrast, when either the transmitter or receiver is highly energy-starved, the two protocols offer almost the same performance. Also, the time-diversity available when the channel is fast fading helps in improving the performance in the scenarios when the harvesting rate is low. In contrast to [16], [17], and [23], we also derive *closed-form* expressions that are exact over a wide range of system parameters. The closed-form expressions, in turn, provide insights into the performance tradeoffs and aid in designing efficient, and near-optimal EH based communication systems.

II. System Model

We consider an EHN which needs to deliver a data packet once in a *frame* of T_m s. to a receiving EHN. Each transmission attempt takes T_p s., including the time the transmitting EHN waits to receive the ACK or NACK. Thus, a frame contains $K \triangleq \lfloor T_m/T_p \rfloor$ slots, which is also the maximum number of possible attempts for a packet, where $\lfloor \cdot \rfloor$ denotes the floor function. A packet is retransmitted until the transmitting EHN receives an ACK, or the frame duration expires. If an ACK is received, the EHNs do not attempt to communicate and accumulate the harvested energy in a finite capacity but otherwise perfectly efficient battery for the rest of the frame. The ACK/NACK messages are assumed to be received without error at the transmitter.

We analyze the packet drop performance with two different retransmission protocols at the link layer: the basic ARQ and the HARQ-CC. In the basic ARQ, for decoding, the receiver uses the packet received in the current attempt only, and discards all the erroneously received copies of

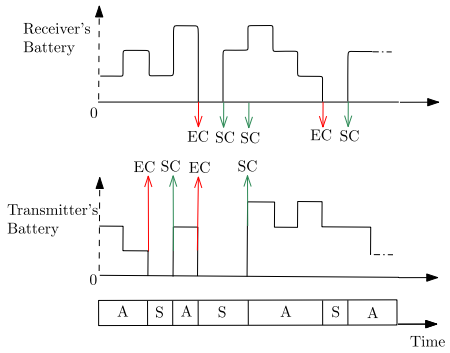

Fig. 1. The coordinated sleep-wake protocol for dual EH links. The (↓) and (↑) arrows indicate that a node is sending a control signal, i.e., an end-communication or start-communication signal. Further, "A" and "S" represent the time intervals during which both nodes are 'awake' and 'sleep', respectively.

the packet. In HARQ-CC, the receiver tries to decode the packet received in the current attempt by maximal ratio combining it with all the previously received copies of the same packet. For basic ARQ, we say that the packet is received in *outage*, if the signal-to-noise ratio (SNR), γ_ℓ, of the packet received in the ℓ^{th} *attempt* is less than the minimum SNR, γ_0, required for successful decoding. For HARQ-CC, the packet remains in outage if the *accumulated* SNR, $\gamma_{ac,\ell}$, up to and including the SNR of the packet received in ℓ^{th} attempt, is less than γ_0. In addition, for both schemes, the packet remains in outage if either the transmitting or receiving EHN does not have sufficient energy to communicate. A packet is *dropped* if it remains in outage till the end of the frame, i.e., if the EHN fails to deliver it successfully within the K transmission opportunities.

To ensure better rendezvous between the EHNs, and for improved energy efficiency, we consider a *coordinated sleep-wake* protocol [30] with the following control signals:

SC: Start-Communication,

EC: End-Communication.

As shown in Fig. 1, the transmitter or receiver sends the end-communication signal if it does not have sufficient energy to participate in communication. For a transmitter, the phrase 'sufficient energy' means having adequate energy to transmit a packet and receive the ACK/NACK message, while for a receiver it means having enough energy to receive and decode a packet, and transmit the ACK/NACK message. If a node receives the end-communication signal in a slot, it goes into 'sleep' mode, as successful communication is not possible. In the sleep mode, a node incurs a very low (effectively zero) energy cost, while it could continue to harvest energy. If a node receives a start-communication signal while in sleep mode, and if it has sufficient energy, it turns on and prepares itself to participate in communication from the start of the next slot. We assume that, for both nodes, the end-communication and start-communication signals are received error free.[1] Since, under the coordinated sleep-wake protocol, an attempt is made only if both nodes have sufficient energy, the coordinated sleep-wake protocol completely avoids the energy wastage that happens if one node tries to communicate when the other node has run out of energy.

We model the EH process at both nodes as a stationary, independent and identically distributed (i.i.d.) Bernoulli process, i.e., at the beginning of every slot, the transmitter harvests energy E_s with probability ρ_t, and with probability $1-\rho_t$, it does not harvest [16], [17], [33]. The harvesting probability at the receiver is denoted by ρ_r. The Bernoulli model, while simple, captures the sporadic and random nature of the EH process and also simplifies the exposition of the key ideas presented in this paper. However, as will be shown later in the paper, the framework presented here can be easily extended to more sophisticated models, such as the stationary Markov model [33], [34] (see Section VII-A) and the generalized Markov model [35], which are appropriate models for solar harvested energy and piezoelectric energy [35], [36], respectively.

We consider an RIP, where the transmitting EHN, in the K attempts, transmits at predetermined power levels given as $\mathcal{P} = \{P_1 \triangleq \frac{L_1 E_s}{T_p}, P_2 \triangleq \frac{L_2 E_s}{T_p}, \ldots, P_K \triangleq \frac{L_K E_s}{T_p}\}$, where $L_\ell \in \mathbb{R}^+$ is the amount of energy used and P_ℓ is transmit power level in the ℓ^{th} transmission attempt[2] of a given packet. Since the prescribed power levels are independent of the instantaneous state-of-charge (SoC) of the battery, the RIPs are suitable for use in scenarios where it is energy-expensive or technologically challenging to accurately estimate the SoC [37]–[39]. Moreover, as will be demonstrated in the sequel, a well designed RIP can even outperform a policy obtained using the Markov decision process (MDP) which uses quantized SoC information (see Fig. 10). The details related to the design of optimal RIPs along with theoretical guarantees on the performance of optimal RIPs are provided in our follow up work [7].

For the receive energy consumption, since the size as well as the modulation and coding scheme for each packet is fixed, i.e., the data rate remains fixed, we adopt a simple model where the node consumes R units of energy to receive a packet and send an ACK/NACK message [19], [23], [40], [41].

The RIPs conform to the energy neutrality constraint through the battery evolution, at the transmitter, given by[3]

$$B^t_{n+1} = \begin{cases} \min(B^t_n + 1 - L_\ell \mathbb{1}_{\{L_\ell \le B^t_n, R \le B^r_n, U_n \neq -1\}}, B^t_{\max}), \\ \qquad \text{if energy is harvested in } n^{\text{th}} \text{ slot}, \\ B^t_n - L_\ell \mathbb{1}_{\{L_\ell \le B^t_n, R \le B^r_n, U_n \neq -1\}}, \\ \qquad \text{if no energy is harvested in } n^{\text{th}} \text{ slot}, \end{cases} \tag{1}$$

where $B^t_{\max}$ is the capacity of the battery at the transmitter, B^t_n and B^r_n denote the battery level in the n^{th} slot at the

[1] The EH-WISP-Mote and REACH-Mote employ a wake-up receiver with an energy harvesting circuit. Node wakeup is feasible at a range of up to 37 ft [30], using wake-up transmitter devices such as an RFID reader [31] or a powercast transmitter [32].

[2] Note: we consider an attempt-based power prescription in this work, not a slot-based prescription. Hence, P_ℓ is the power used in the ℓ^{th} attempt, not the ℓ^{th} slot within a frame.

[3] Throughout the paper, the battery levels such as B^t_n, B^r_n, $B^t_{\max}$, $B^r_{\max}$, are normalized with respect to E_s. Further, for the foregoing Markov chain formulation, we require that the power levels such as L_ℓ and R are integer or fractional-valued.

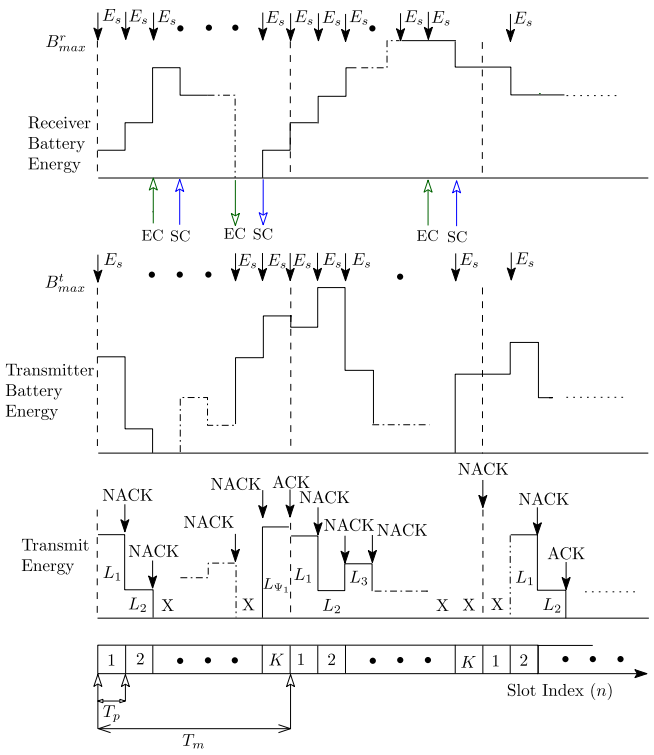

Fig. 2. Communication time-line of the EHN, showing the random energy harvesting moments and periodic data arrivals. The marker "X" denotes the slots where the EHN does not communicate due to insufficient energy, and L_{Ψ_1} denotes the power level of the last attempt, i.e., there are Ψ_1 feasible attempts in the frame.

transmitter and receiver, respectively, and $U_n \in \{-1, 1 \ldots, K\}$ denotes the packet attempt index. Starting from $U_n = 1$ at the beginning of the frame, it is incremented by 1 after each unsuccessful attempt, and set to -1 for the rest of the frame, once an ACK is received. Thus, (1) is written using the fact that, under the coordinated sleep-wake protocol, if the transmitter has not yet received an ACK for the current packet, the ℓ^{th} attempt is made in the n^{th} slot if and only if $B^t_n \geq L_\ell$ and $B^r_n \geq R$. At the receiver, the battery evolves in a similar fashion, and the evolution is given by

$$B^r_{n+1} = \begin{cases} \min(B^r_n + 1 - R\mathbb{1}_{\{L_\ell \leq B^t_n, R \leq B^r_n, U_n \neq -1\}}, B^r_{\max}), \\ \qquad \text{if energy is harvested in } n^{\text{th}} \text{ slot}, \\ B^r_n - R\mathbb{1}_{\{L_\ell \leq B^t_n, R \leq B^r_n, U_n \neq -1\}}, \\ \qquad \text{if no energy is harvested in } n^{\text{th}} \text{ slot}, \end{cases}$$

After an ACK is received, both nodes accumulate the harvested energy for the rest of the frame. Fig. 2 illustrates the battery evolution of the EHN with random energy injections.

We consider a *block* fading wireless channel between the transmitter and receiver in both slow and fast fading cases. The *slow* fading channel remains constant for the duration of a frame, and changes in an i.i.d. fashion from one frame to the next, while the *fast* fading channel stays constant for a slot, and varies in an i.i.d. fashion from slot to slot. The transmitter only has access to implicit CSI, obtained from the ACK/NACK messages. In both cases, the channel is assumed to be Rayleigh distributed, with the complex baseband channel distributed as $\mathcal{CN}(0, \sigma_c^2)$. As described earlier, for the basic ARQ protocol, a packet remains in outage in the ℓ^{th} attempt, if $\gamma_\ell = \frac{P_\ell |h_\ell|^2}{\mathcal{N}_0} < \gamma_0$, where $|h_\ell|^2$ represents the channel gain during the ℓ^{th} attempt and $\mathcal{N}_0$ denotes the power spectral density of the additive white Gaussian noise at the receiver. Hence, for the Rayleigh fading channel, the probability that the ℓ^{th} attempt results in an outage is given as

$$p_{\text{out},\ell} \triangleq \Pr[\gamma_\ell < \gamma_0] = 1 - e^{-\frac{\gamma_0 \mathcal{N}_0 T_p}{L_\ell E_s \sigma_c^2}}, \tag{2}$$

In HARQ-CC, a packet received in a given attempt is decoded by maximal ratio combining it with the copies of the packet received in all previous attempts. Since MRC corresponds to weighing each copy of the received packet with the complex conjugate of the overall gain applied to the data symbols (including the effect of the power level prescribed by the RIP), the output SNR of MRC is simply the accumulated SNR of the packets received so far. Hence, for HARQ-CC, in the ℓ^{th} attempt, the packet remains in outage if the accumulated SNR, $\gamma_{ac,\ell}$, up to and including the SNR of the packet received in the current round is less than γ_0. As a result, for the EH link with a chase combining receiver, the probability that the packet remains in outage is written as

$$p_{\text{out},1\to\ell} \triangleq \Pr[\gamma_{ac,\ell} < \gamma_0], \text{ where } \gamma_{ac,\ell} = \sum_{i=1}^{\ell} \frac{P_i |h_i|^2}{\mathcal{N}_0}. \tag{3}$$

Note that, $p_{\text{out},0} = 1$ and $p_{\text{out},1\to 0} = 1$.

A packet is dropped if all the attempts result in outage. For ARQ, informally, the PDP is $P_{\text{D}} = \Pr\left[\cap_{\ell=1}^{\ell_m} (\gamma_\ell < \gamma_0)\right]$, while for HARQ-CC it is $P_{\text{D}} = \Pr[\gamma_{ac,\ell_m} < \gamma_0]$, where ℓ_m denotes the index of the *last* attempt in the frame. The PDP depends on ℓ_m, whose distribution is difficult to characterize, as it has a complex dependence on the energy harvesting and channel dynamics, the battery capacities at the transmitter and receiver, etc. In the next section, using a Markov chain formulation, we analyze the PDP of the above described system, which is the main result of the paper.

III. PDP Analysis of Dual EH Links

In this section, we analyze the PDP of dual EH links with ARQ and HARQ-CC. Since the battery states at both nodes evolve in a Markovian fashion, the system evolution within a frame is modeled as a discrete time Markov chain (DTMC). The state of the system consists of the battery states at the EHNs and the packet attempt index. The PDP can be obtained by averaging the PDP conditioned on the system state over its stationary distribution. To this end, we derive the conditional PDP and stationary distribution, for both ARQ and HARQ-CC, and for both slow and fast fading channels. We proceed by describing the formulation of the DTMC in the following.

As shown in Fig. 3, the state of this DTMC is represented by a tuple (B^t_n, B^r_n, U_n), where B^t_n and B^r_n are the battery state at the transmitter and receiver, respectively, and $U_n \in \{-1, 1, \ldots, K\}$ represents the *packet attempt index* in the n^{th} slot, defined as

$$U_n \triangleq \begin{cases} -1 & \text{ACK received}, \\ \ell & \ell - 1 \text{ NACKs received}, \quad \ell \in \{1, \ldots, K\}. \end{cases} \tag{4}$$

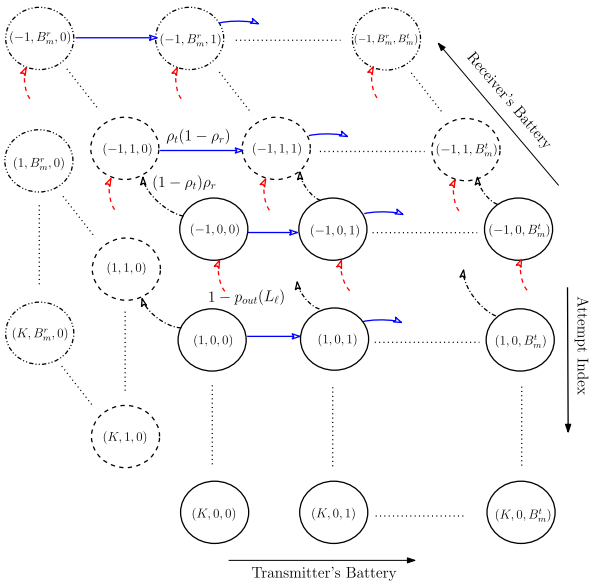

Fig. 3. DTMC for an RIP. The energy states are normalized with respect to E_s. B_m^t and B_m^r denote the capacity of the battery at the transmitter and receiver, respectively. In the above figure, only feasible transitions are depicted. For example, $(K,0,0) \to (K,1,1)$ and $(1,0,0) \to (-1,0,0)$ are not feasible transitions. The transition probabilities of this DTMC are given in Appendix A.

A packet is dropped if and only if $U_K \neq -1$, i.e., if the transmitter does not receive an ACK by the end of the frame.

The state transition probability matrix (TPM) of the DTMC is denoted by $\boldsymbol{G}$. The elements of $\boldsymbol{G}$ represent the probability of a transition from state (i_1, j_1, ℓ_1) to state (i_2, j_2, ℓ_2) in a single slot, and are defined as

$$G_{i_1,j_1,\ell_1}^{i_2,j_2,\ell_2} \triangleq \Pr\Big[(B_{n+1}^t = i_2, B_{n+1}^r = j_2, U_{n+1} = \ell_2) \Big| (B_n^t = i_1, B_n^r = j_1, U_n = \ell_1)\Big]. \quad (5)$$

The transition probabilities are determined by the RIP $\mathcal{P}$, and the statistics of the channel and the EH processes at the EHNs. In contrast to mono EH links [16], [17], the transition probabilities of dual EH links need to account for the possible correlation of the EH processes and the coupled evolution of the batteries at the nodes. The transition probabilities are provided in Appendix A.

Remark 1: The events that a node sends an start-communication or end-communication signal are implicitly accounted for in the transition probabilities. For example, when $i_1 < L_\ell$ (or $j_1 < R$), the transition probabilities do not include a $p_{\text{out},\ell}$ term, thus accounting for an end-communication signal sent by the transmitter (or receiver).

Now, for any given RIP $\mathcal{P}$, the average packet drop probability is given by

$$P_{\text{D}}(K) = \sum_{i,j} \pi(i,j) P_{\text{D}}(K|i,j,\ell=1). \quad (6)$$

Thus, to compute the PDP, we average the conditional PDP, $P_{\text{D}}(K|i,j,\ell=1)$, over the stationary distribution, $\boldsymbol{\pi}$, of the Markov chain, where $\pi(i,j)$ denotes the stationary probability that the transmitter and receiver have (iE_s, jE_s) energy at the start of the frame. The conditional probability, $P_{\text{D}}(K|i,j,\ell=1)$, denotes the probability that the packet is dropped given that the battery states of the transmitter and receiver at the beginning of the frame are i and j, respectively, where $(i,j) \in \{(i_t, j_r) \mid 0 \le i_t \le B_{\max}^t, 0 \le j_r \le B_{\max}^r\}$, and conditioning on the attempt index $\ell = 1$ indicates the start of the frame.

To obtain the PDP using (6), we need to find the stationary distribution, $\boldsymbol{\pi}$, and the conditional PDP, $P_{\text{D}}(K|i,j,\ell=1)$. Existence of the stationary distribution is ensured by the fact that the number of states is finite, since both the EHNs have finite capacity batteries, and therefore the DTMC is positive recurrent. Next, we derive the stationary distribution for both ARQ and HARQ-CC, with both slow and fast fading channels.

A. Derivation of the Stationary Distribution

The stationary probabilities, $\pi(i,j)$, that the transmitter and receiver have (iE_s, jE_s) units of energy at the *start* of the frame is given by [42, Lemma 1]

$$\boldsymbol{\pi} = (\boldsymbol{G'} - \boldsymbol{I} + \boldsymbol{B})^{-1}\boldsymbol{b} \quad (7)$$

where $\boldsymbol{b} = (1,\ldots,1)^T \in \mathbb{R}^{(B_{\max}^t+1)(B_{\max}^r+1)}$, $\boldsymbol{B}_{i,j} = 1 \; \forall \; i,j$, and $\boldsymbol{G'}$ is the K-step TPM of battery states with its entries $\Pr\Big[\Big(B_{(M+1)K}^t = i_2, B_{(M+1)K}^r = j_2\Big) \Big| \Big(B_{MK}^t = i_1, B_{MK}^r = j_1\Big)\Big]$, where M denotes the frame index, for all (i_1, i_2, j_1, j_2). We use the TPM, $\boldsymbol{G}$, to compute $\boldsymbol{G}^K$. The entries of $\boldsymbol{G}^K$ are in turn used to compute the entries of $\boldsymbol{G'}$ as:

$$\sum_{u\in\{-1,1,\ldots,K\}} \Pr\Big[\Big(B_{(M+1)K}^t = i_2, B_{(M+1)K}^r = j_2, U_{(M+1)K} = u\Big) \Big| \Big(B_{MK}^t = i_1, B_{MK}^r = j_1, U_{MK} = 1\Big)\Big]. \quad (8)$$

In next subsection, we derive the expressions for the conditional PDP of dual EH links.

B. Exact Conditional PDP of Dual EH Links With ARQ

The key technical challenge in deriving the conditional PDP of dual EH links is that for a given RIP $\mathcal{P}$ and battery states (i,j) at the beginning of the frame, the conditional PDP, $P_{\text{D}}(K|i,j,\ell=1)$, depends on the evolution of the battery at the transmitter and receiver, which, in turn, depends on the harvesting instances at both EHNs and their battery states. In the following, we derive an exact expression for the conditional PDP. For the clarity of exposition, the conditional PDP is derived for mutually i.i.d. harvesting processes. However, the result can be extended to incorporate both the spatial and temporal correlation of the harvesting processes (see Sec. VII).

Lemma 1: For ARQ-based dual EH links with i.i.d. Bernoulli harvesting processes at the transmitter and receiver with harvesting probabilities ρ_t and ρ_r, the conditional PDP, $P_{\text{D}}(K|i,j,\ell)$, for all $\ell \ge 1$ and $K \ge 1$, is given by the recursive expression in (9)*, as shown at the bottom of the next page.*

Proof: When $i \geq L_\ell, j \geq R$, both the transmitter and receiver have sufficient energy to make ℓ^{th} transmission attempt. Depending on the four mutually exclusive cases where the transmitter, receiver, both, or neither harvest energy in the first slot, we get the four terms in the expression for the case $i \geq L_\ell, j \geq R$, with $P_{\text{D}}(0|i, j, \ell) = 1$ for all values of i, j and ℓ. Specifically, the first term denotes the probability that the packet is dropped after K slots given that the ℓ^{th} attempt is feasible and both transmitter and receiver harvest energy in the first slot. It is written as a product of three terms: the probability of outage in ℓ^{th} attempt, the probability that both transmitter and receiver harvest energy in the first slot, and the conditional PDP, $P_{\text{D}}(K-1|i-L_\ell+1, j-R+1, \ell)$. The conditional PDP, $P_{\text{D}}(K-1|i-L_\ell+1, j-R+1, \ell)$, is the probability that the packet is dropped after the remaining $K-1$ slots given that the batteries of the transmitter and receiver have evolved to $i-L_\ell+1$ and $j-R+1$, respectively. Other three terms in the sum are written similarly. Also, the cases $i < L_\ell$ and $j < R$ are handled by a similar reasoning, by observing the fact that, in these cases, the packet cannot be attempted in the first slot. ∎

A similar expression for $P_{\text{D}}(K|i, j, \ell)$ of dual EH links with HARQ-CC can be obtained, with replacing $p_{\text{out},\ell}$ in (9) with $p_{\text{out},1\to\ell}$ given by (3). This completes the characterization of the exact conditional PDP and stationary distribution, which can in turn be used to compute the PDP of dual EH links using (6), (7) and (9). In the next subsection, we summarize the procedure to compute the PDP.

C. Procedure to Compute the PDP

The procedure to compute the PDP is summarized in Algorithm 1. We note that the algorithm provides an easy-to-use recipe for finding the exact PDP of dual EH links.

The PDP obtained using the conditional PDP in (9) is in recursive form, which does not offer insights into the effect of various system parameters on the PDP. In the next section, we derive closed-form expressions for the conditional PDP of dual EH links.

IV. Closed Form Expressions for the PDP of Dual EH Links

As can be observed from (9), for a given initial state (i, j) of the battery at the transmitter and receiver, the exact conditional PDP $P_{\text{D}}(K|i, j, \ell = 1)$ depends not only on the number of slots but also on the slot index in which energy is harvested. Due to this, it is required to keep track of the battery state to compute the exact PDP, which, in turn, results in the recursive expression in (9). However, the following key observations allow us to obtain a closed-form expression which is exact in a wide range of practical scenarios:

1) The conditional PDP depends only on the number of feasible attempts in the frame, and not on the slot indices when the attempts are made.
2) In general, for a given battery state tuple, (i, j), the number of feasible attempts is determined by the exact slot indices in which energy is harvested and depleted. However, for a system with sufficiently large battery at the EHNs (such that the energy overflow can be neglected), the number of feasible attempts depends only on the *number* of slots in which energy is harvested, and not on the precise energy arrival and departure instants. This observation is also valid for any RIP for which $L_\ell \geq 1$ for all $1 \leq \ell \leq K$.

Using these observations, we can write the conditional PDP as a function of the initial battery state tuple (i, j) and the number of slots in which energy is harvested. Let $p_{\text{D}}(i, j, m_t, m_r)$ denote the PDP of dual EH links when the transmitter and receiver have i and j units of energy at the start of the frame and harvest m_t and m_r units of energy during the frame, respectively. The following Lemma provides a closed form expression for the conditional PDP of dual EH links in terms of $p_{\text{D}}(i, j, m_t, m_r)$. We omit the proof as it is straightforward.

Lemma 2: For dual EH links with mutually i.i.d. Bernoulli harvesting processes at the transmitter and receiver with harvesting probabilities ρ_t and ρ_r, the conditional PDP,

Algorithm 1 Procedure to Compute the PDP

1: Compute $\boldsymbol{G}$ from (32) in Appendix A, and the K-step TPM, $\boldsymbol{G}^K$.
2: Using the entries of $\boldsymbol{G}^K$, compute $\boldsymbol{G}'$ in (7) using (8).
3: Calculate the stationary probabilities, $\pi(i, j)$, using (7).
4: Calculate the conditional probabilities $P_{\text{D}}(K|i, j, \ell = 1)$ using (9).
5: Calculate the PDP $P_{\text{D}}(K)$ by substituting the results from steps 3 and 4 in (6).

$$P_{\text{D}}(K|i, j, \ell) = \begin{cases} p_{\text{out},\ell}\,[\rho_t\rho_r P_{\text{D}}(K-1|i-L_\ell+1, j-R+1, \ell+1) \\ +\rho_t(1-\rho_r)P_{\text{D}}(K-1|i-L_\ell+1, j-R, \ell+1) \\ +(1-\rho_t)\rho_r P_{\text{D}}(K-1|i-L_\ell, j-R+1, \ell+1) \\ +\ (1-\rho_t)(1-\rho_r)P_{\text{D}}(K-1|i-L_\ell, j-R, \ell+1)], & i \geq L_\ell, j \geq R, \\ \rho_t\rho_r P_{\text{D}}(K-1|i+1, j+1, \ell) \\ +\rho_t(1-\rho_r)P_{\text{D}}(K-1|i+1, j, \ell) \\ +(1-\rho_t)\rho_r P_{\text{D}}(K-1|i, j+1, \ell) \\ +(1-\rho_t)(1-\rho_r)P_{\text{D}}(K-1|i, j, \ell), & i < L_\ell \text{ or } j < R, \end{cases} \tag{9}$$

where $p_{\text{out},\ell}$ is given by (2) and $P_{\text{D}}(0|i, j, \ell) = 1$ for all values of i, j and ℓ.

$P_D\,(K|i,\,j,\,\ell=1)$, can be written as

$$P_{\rm D}(K|i,\,j,\,\ell=1)=\sum_{m_t=0}^{K}\sum_{m_r=0}^{K}\binom{K}{m_t}\binom{K}{m_r}\rho_t^{m_t}\rho_r^{m_r}$$
$$(1-\rho_t)^{K-m_t}(1-\rho_r)^{K-m_r}\,p_{\rm D}(i,\,j,\,m_t,\,m_r),\qquad(10)$$

In the above, the calculation of $p_{\rm D}(i,\,j,\,m_t,\,m_r)$ depends on the type of retransmission protocol and whether the channel is slow or fast fading. In next subsection, we derive expressions for $p_{\rm D}(i,\,j,\,m_t,\,m_r)$ for ARQ-based dual EH links over both slow and fast fading channels.

A. Dual EH Links With ARQ

First, we discuss the case of slow fading channels. For slow fading channels, since the channel is constant over the frame, if the packet remains in outage at a particular power level, all future attempts of the packet at the same or lower power level will also remain in outage. Hence, without loss of generality, we can assume that $P_1<P_2<\cdots<P_K$. For such policies, $p_{\rm D}(i,\,j,\,m_t,\,m_r)$ depends on the power level of the *last feasible* attempt (which, in turn, is determined by the tuple $(i,\,j,\,m_t,\,m_r)$). This is stated in the next Lemma.

Lemma 3: For dual EH links with ARQ and slow fading channels, $p_D(i,\,j,\,m_t,\,m_r)=p_{out,\Psi_1}$, where p_{out,Ψ_1} is given by (2), and for a given policy $\mathcal{P}$ such that $P_1<P_2<\cdots<P_K$, $0\le\Psi_1\le K$ denotes the number of feasible attempts for the tuple $(i,\,j,\,m_t,\,m_r)$.

Proof: Since $P_1<P_2<\cdots<P_K$, we write

$$p_{\rm D}(i,\,j,\,m_t,\,m_r)=\Pr\left\{\bigcap_{\ell=1}^{\Psi_1}\left(|h|^2<\frac{\gamma_0\mathcal{N}_0}{P_\ell}\right)\right\},$$
$$=\Pr\left\{\left(|h|^2<\frac{\gamma_0\mathcal{N}_0}{P_{\Psi_1}}\right)\right\}=p_{{\rm out},\Psi_1}.\qquad(11)$$

■

In the above Lemma, the outage probability depends on Ψ_1, the number of feasible transmission attempts (or L_{Ψ_1}) in a frame. This, in turn, depends on the energy available in the frame, which is a function of the battery states at the beginning of the frame, $(i,\,j)$, as well as on the number of slots in which the energy is harvested and stored in the battery. In general, the available energy depends on the order in which energy arrives and is used. Let the total energy available at the transmitter and receiver in a frame be denoted by $E^t_{\rm avl}$ and $E^r_{\rm avl}$, respectively. The following Lemma provides an expression for the number of attempts, Ψ_1, in terms of $E^t_{\rm avl}$ and $E^r_{\rm avl}$.

Lemma 4: For a given policy $\mathcal{P}=\{P_1,\,P_2,\,\ldots,\,P_K\}$,

$$\Psi_1=\min\{\kappa_t,\,\kappa_r\},\qquad(12)$$

where

$$\kappa_t\triangleq\max\{\ell|1\le\ell\le K,\,E^t_{\rm avl}-\sum_{k=1}^{\ell}P_kT_p\ge0\},\qquad(13)$$

$$\kappa_r\triangleq\max\{\ell|1\le\ell\le K,\,E^r_{\rm avl}-\ell R\ge0\}.\qquad(14)$$

Here, κ_t and κ_r denote the number of feasible attempts in the current frame at the transmitter and receiver, respectively.

Proof: Equation (12) follows from the operation of the coordinated sleep-wake protocol, while (13) and (14) follow from the energy neutrality constraint. ■

Next, for a given initial battery level and amount of energy harvested at the transmitter and receiver, we propose an approximation for $E^t_{\rm avl}$ and $E^r_{\rm avl}$. Due to the randomness in the energy arrivals and uses, $E^t_{\rm avl}(i,m_t)$ and $E^r_{\rm avl}(j,m_r)$ are random variables, taking values $i\le E^t_{\rm avl}(i,m_t)\le i+m_t$ and $j\le E^r_{\rm avl}(j,m_r)\le j+m_r$. We approximate the $E^t_{\rm avl}$ and $E^r_{\rm avl}$ as $\min\{i+m_t,\,B^t_{\max}\}$ and $\min\{j+m_r,\,B^r_{\max}\}$, respectively. In general, this approximation provides a lower bound on $E^t_{\rm avl}$ and $E^r_{\rm avl}$, which can potentially result in underestimation of number of feasible attempts, Ψ_1. However, the next Lemma asserts that, in a scenario when the size of the battery at the EHNs is sufficient to store the energy needed to support all K attempts in a frame, there is no error in the above approximation. It also provides an exact expression for $E^t_{\rm avl}$ and $E^r_{\rm avl}$ in a scenario when $R\ge1$ and $L_\ell\ge1$ for all $1\le\ell\le K$.

Lemma 5: In a given frame, let i and j be the initial battery states, and m_t and m_r be the number of slots where energy is harvested, at the transmitter and receiver, respectively.

i) Consider a power control policy such that $\sum_{\ell=1}^{K}L_\ell\le B^t_{max}$ and $KR\le B^r_{max}$. Then, the number of feasible attempts, Ψ_1, computed using the approximations $E^t_{avl}\approx\min\{i+m_t,\,B^t_{max}\}$ and $E^r_{avl}\approx\min\{j+m_r,\,B^r_{max}\}$ are accurate.

ii) Also, consider a policy such that $L_\ell\ge1$ for all $1\le\ell\le K$ and $R\ge1$. Then, $E^t_{avl}=i+m_t$ and $E^r_{avl}=j+m_r$.

Proof: See Appendix B. ■

This completes the computation of the PDP in closed-form. In the scenarios mentioned in the above Lemma, the computed PDP is *exact*. However, when the hypotheses on the power control policy in the above Lemma do not hold, the above approximations are a lower bound on the available energy, $E^t_{\rm avl}$ and $E^r_{\rm avl}$, which results in an underestimation of the number of feasible attempts. Hence, in general, the PDP computed using these closed-form expressions serve as an *upper bound* on the actual PDP.

We next turn to the case of *fast fading* channels, and provide an expression for $p_{\rm D}(i,\,j,\,m_t,\,m_r)$ in the next Lemma.

Lemma 6: For fast fading channels, $p_D(i,\,j,\,m_t,\,m_r)$ simplifies as

$$p_{\rm D}(i,\,j,\,m_t,\,m_r)=\prod_{\ell=1}^{\Psi_1}p_{{\rm out},\ell},\qquad(15)$$

where Ψ_1 is given by (12).

Proof: In the fast fading case, since the channel is i.i.d. from slot to slot, $p_{\rm D}(i,\,j,\,m_t,\,m_r)$ is the product of the outage probabilities of all the individual attempts. ■

From Lemmas 3 and 6, it is evident that for a given policy, slow fading channels result in a higher $p_D(i,\,j,\,m_t,\,m_r)$ compared to fast fading channels. Hence, a given PDP can be achieved at a significantly lower harvesting rate when the channel is fast fading compared to the case when it is slow fading (see Figs. 5 and 6). In Sec. V-D, for dual EH links operating in the EUR, we provide an expression for the

performance gain of fast fading channels over slow fading channels.

B. Dual EH Links With HARQ-CC

To obtain closed-form expressions for the PDP of dual EH links with HARQ-CC, we use (10), which requires us to determine $p_{\mathrm{D}}(i, j, m_t, m_r)$. With HARQ-CC, $p_{\mathrm{D}}(i, j, m_t, m_r)$ is written as

$$p_{\mathrm{D}}(i, j, m_t, m_r) = \Pr\left[\frac{\sum_{\ell=1}^{\Psi_1} P_\ell |h_\ell|^2}{\mathcal{N}_0} < \gamma_0\right], \tag{16}$$

where Ψ_1 is given by (12). For *slow fading* channels,

$$\begin{aligned} p_{\mathrm{D}}(i, j, m_t, m_r) &= \Pr\left[|h|^2 < \frac{\gamma_0 \mathcal{N}_0}{\sum_{\ell=1}^{\Psi_1} P_\ell}\right], \\ &= 1 - e^{-\frac{\gamma_0 \mathcal{N}_0}{\sigma_c^2 \sum_{\ell=1}^{\Psi_1} P_\ell}}, \end{aligned} \tag{17}$$

where (17) is written using (3). For *fast fading* channels

$$p_{\mathrm{D}}(i, j, m_t, m_r) = \Pr\left[\sum_{\ell=1}^{\Psi_1} L_\ell |h_\ell|^2 < \frac{\gamma_0 \mathcal{N}_0 T_p}{E_s}\right]. \tag{18}$$

In the above equation, $\sum_{\ell=1}^{\Psi_1} L_\ell |h_\ell|^2$ is a sum of independent and non-identically distributed exponential random variables. The $p_{\mathrm{D}}(i, j, m_t, m_r)$ can be written as [5]

$$\begin{aligned} p_{\mathrm{D}}(i, j, m_t, m_r) = 1 - &\sum_{s=1}^{M_{\Psi_1}} \sum_{t=1}^{\tau_s} \sum_{k=0}^{t-1} \frac{\chi_{s,t}(\mathbf{L}_{\Psi_1})}{k!} \left(\frac{X}{L_{\{s\}}}\right)^k \\ &\times e^{-\left(\frac{X}{L_{\{s\}}}\right)}, \end{aligned} \tag{19}$$

where $X = \frac{\gamma_0 \mathcal{N}_0 T_p}{E_s}$, $\mathbf{L}_{\Psi_1} = \mathrm{diag}(\frac{L_1}{\sigma_c^2}, \frac{L_2}{\sigma_c^2}, \ldots, \frac{L_{\Psi_1}}{\sigma_c^2})$, and M_{Ψ_1}, $1 \le M_{\Psi_1} \le \Psi_1$ is the number of distinct nonzero elements of $\mathbf{L}_{\Psi_1}$. $L_{\{1\}}, L_{\{2\}}, \cdots, L_{\{M_{\Psi_1}\}}$ denote the distinct nonzero elements of $\mathbf{L}_{\Psi_1}$, and τ_s denotes the multiplicity of $L_{\{s\}}$. Note that Ψ_1 is a function of (i, j, m_t, m_r), given by (12). Here, $\chi_{s,t}(\mathbf{L}_{\Psi_1})$ denotes the $(s,t)^{\text{th}}$ characteristic coefficient of $\mathbf{L}_{\Psi_1}$ such that

$$\begin{aligned} \det(\mathbf{I} + u\mathbf{L}_{\Psi_1})^{-1} &= \frac{1}{(1 + uL_{\{1\}})^{\tau_1} \cdots (1 + uL_{\{M_{\Psi_1}\}})^{\tau_{M_{\Psi_1}}}}, \\ &= \sum_{s=1}^{M_{\Psi_1}} \sum_{t=1}^{\tau_s} \frac{\chi_{s,t}(\mathbf{L}_{\Psi_1})}{(1 + uL_{\{s\}})^t}, \end{aligned} \tag{20}$$

where u is a scalar satisfying $\det(\mathbf{I} + u\mathbf{L}_{\Psi_1}) \neq 0$. In the general case, $\chi_{s,t}(\mathbf{L}_{\Psi_1})$ is given by (21), shown at the bottom of the page, where $\omega_{s,t} = \tau_s - t$. In the above, (19) simplifies in the special cases of *equal* power and *distinct* power policies. The simplified expressions, as well as details on the derivation of the above result, are presented in [5].

Thus, the outage probability, $p_D(i, j, m_t, m_r)$, of HARQ-CC depends on the number of realizable attempts, Ψ_1, which, in turn, depends on the EH profiles, the policy $\mathcal{P}$, and the energy required for decoding. We discuss the performance gain of HARQ-CC over ARQ and provide further insights in the next section.

Substituting the expressions for $p_{\mathrm{D}}(i, j, m_t, m_r)$ derived above into the conditional PDP $P_D(K|i,\ j, \ell = 1)$ in (10), we can now compute the PDP using (6) and (7). This completes the PDP analysis of dual EH links for both ARQ and HARQ-CC, with both slow and fast fading channels.

In some applications, such as body area networks, an EHN may be a battery-less node [43], while in other applications the battery can be very large (practically infinite). In the next section, we show how our framework can be used to obtain closed-form expressions for the PDP and discuss the insights obtained from the analysis of these special cases.

V. Special Cases: Zero and Infinite Battery

A. Dual EH Links With Battery-Less EHNs

The PDP analysis of a node with *zero energy buffer* can be obtained as a special case of the above analysis by setting $B_n^t = B_n^r = 0$ for all n, and $E_s = PT_p$ and $R \le 1$, as for a battery-less node it is optimal to use all the harvested energy immediately. Hence, the PDP for slow fading channels is given by

$$P_{\mathrm{D}}(K) = 1 - \left(1 - (1 - \rho_t \rho_r)^K\right) e^{-\frac{\gamma_0 \mathcal{N}_0 T_p}{E_s \sigma_c^2}}, \tag{22}$$

where (22) is written using (2). The PDP of EH links with battery-less nodes in the other cases, i.e., ARQ with fast fading channel and with HARQ-CC, can be obtained similarly, and the corresponding expressions are provided in [44].

B. Dual EH Links With Infinite Batteries: The Energy Unconstrained Regime

The PDP of dual EH links with infinite capacity batteries at both the EHNs is determined by the statistics of the EH process, the wireless channel, and the transmit and receive power policies. Here, we characterize the conditions under which the randomness in the EH process does not affect the PDP of the system. We call it the *energy unconstrained regime* (EUR). In the EUR, we can obtain simplified expressions for the PDP.

A dual EH link with infinite energy buffers at the nodes operates in the EUR if, at each node, the average energy harvested per frame is greater than the average energy consumed

$$\chi_{s,t}(\mathbf{L}_{\Psi_1}) = \left(\frac{-1}{L_{\{s\}}}\right)^{\omega_{s,t}} \sum_{\substack{k_1 + \cdots + k_{M_{\Psi_1}} = \omega_{s,t} \\ k_s = 0 \\ k_n \in \{0, \omega_{s,t}\} \text{ for } n \neq s}} \left\{ \prod_{\substack{n=1 \\ n \neq s}}^{M_{\Psi_1}} \binom{\tau_n + k_n - 1}{k_n} \left(\frac{L_{\{n\}}^{k_n}}{\left(1 - \frac{L_{\{n\}}}{L_{\{s\}}}\right)^{\tau_n + k_n}}\right) \right\}, \tag{21}$$

per frame. When this happens, the battery state executes a random walk with positive drift. As a consequence, over time, the available energy grows unboundedly, and the node is able to make all its transmission/reception attempts. Also, in this case, the coordinated sleep-wake protocol is not necessary.

Under our EH model, the expected energy harvested per frame at the transmitter and receiver are $K\rho_t E_s$ and $K\rho_r E_s$, respectively. Now, for *slow fading channels*, the average energy consumed at the transmitter and receiver are given by

$$E^c_{\text{av}_t} = \sum_{\ell=1}^{K} p_{\text{out},\ell-1} L_\ell E_s, \tag{23}$$

$$E^c_{\text{av}_r} = \sum_{\ell=1}^{K} \mathbb{1}_{\{L_\ell>0\}} p_{\text{out},\ell-1} R E_s, \tag{24}$$

respectively, where $\mathbb{1}_{\{L_\ell>0\}}$ is an indicator variable which is one when $L_\ell > 0$, and equals zero otherwise; and $p_{\text{out},\ell-1}$ is given by (2). Here, (23) is written using the fact that if the packet is transmitted at energy level L_ℓ is not successful, it is transmitted at power level $L_{\ell+1}$ in the next attempt, and so on. Hence, for slow fading channels, the EH link operates in the EUR if

$$\frac{1}{K}\sum_{\ell=1}^{K} p_{\text{out},\ell-1} L_\ell < \rho_t, \tag{25}$$

$$\frac{R}{K}\sum_{\ell=1}^{K} \mathbb{1}_{\{L_\ell>0\}} p_{\text{out},\ell-1} < \rho_r. \tag{26}$$

For the other cases, conditions under which the system operates in the EUR can be obtained similarly; but the expressions are omitted due to lack of space. Next, we derive the PDP of EH links with infinite buffers.

C. Packet Drop Probability in the Energy Unconstrained Regime

As mentioned earlier, in the EUR, the battery states at the transmitter and receiver have a net positive drift, and over time, accumulate infinite energy. Hence, all K transmission attempts are possible. Thus, in the EUR, the PDP of dual EH links with infinite capacity batteries can be obtained by setting $\Psi_1 = K$ in Lemma 3, (15), (17), and (19). Note that, in this case, the PDP is equal to the conditional PDP.

Fig. 4 illustrates the EUR for ARQ-based links with a slow fading channel. As can be seen from the figure, in practice, an EH link with moderately sized energy buffers (e.g., $B^t_{\max} \approx 12E^c_{\text{av}_t}$ or $10E_s$) can also operate in the EUR, at almost the same values of harvesting probability as for the infinite energy buffer case. Roughly, the probability that batteries at both nodes are in a state (i, j) in which K attempts can be made irrespective of the number of harvesting slots m_t and m_r is close to unity. A rigorous analysis of the achievability of the EUR for finite capacity batteries requires the use of tools from random walks and martingales, and will be presented in our follow up work. In the next subsection, we discuss the insights obtained from the closed-form PDP expression derived in Sec. IV, when the dual EH link is operating in the EUR.

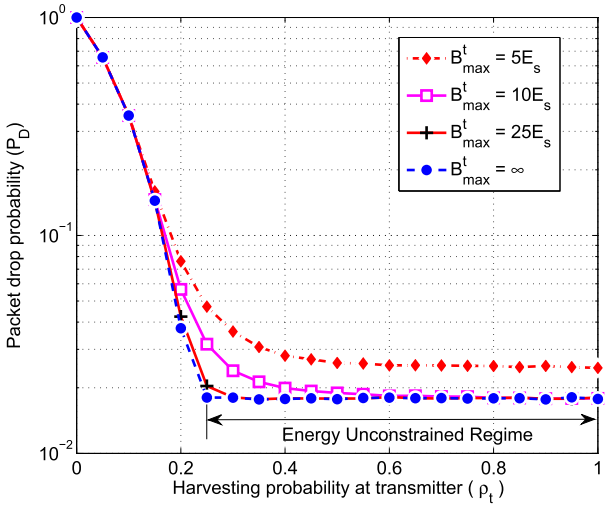

Fig. 4. Illustration of the EUR in slow fading channels with ARQ. The average energy consumed per frame is $E^c_{\text{av}_t} \approx 0.83E_s$. The transmission policy used is [0.5 1.5 2.5 3.5]. The parameters chosen are $\gamma_0 = 10$ dB, $E_s = 15$ dB, and $K = 4$. The simulations are done for a slow fading channel and $\rho_r = 1$.

D. Discussion on the PDP of Dual EH Links in the EUR

In this subsection, we consider ARQ-based dual EH links equipped with finite sized batteries, and we first compare the performance under slow fading with that under fast fading.

For the battery states (i, j) where $\Psi_1 = K$ attempts are feasible, using Lemmas 3 and 6, it can be deduced that the $p_{\text{D}}(i, j, m_t, m_r)$ takes the values $p_{\text{out},K}$ and $\prod_{\ell=1}^{K} p_{\text{out},\ell}$ for slow and fast fading channels, respectively. Hence, using (6), the PDP of slow and fast fading channels can be approximated as $p_{\text{out},K}$ and $\prod_{\ell=1}^{K} p_{\text{out},\ell}$, respectively. Thus, for dual EH links with the ARQ protocol, when the power policy $\mathcal{P}$ allows the link to operate in the EUR, the difference in the PDP of slow and fast fading channels is given by

$$\Delta P_{\text{D}} = p_{\text{out},K}\left(1 - \prod_{\ell=1}^{K-1} p_{\text{out},\ell}\right).$$

For slow fading channels with ARQ, it is better to use a policy that makes a single attempt with high power, while for fast fading channels, using an equal power transmit policy will result in a lower PDP. Using similar arguments, one can deduce that for dual EH links with HARQ-CC and slow fading channels, the PDP of a policy $\mathcal{P}$ depends only on the accumulated energy $\sum_{\ell=1}^{K} L_\ell$, and not on the individual attempt energy levels. One can obtain similar insights for dual EH links with fast fading channels with HARQ-CC operating in the EUR.

In the next section, we show that the framework presented in Sec. III naturally extends to mono EH links, where one node is an EHN while the other node is connected to the mains or is operating in the EUR. We also show that the PDP analysis for mono-T links presented in [16] and [17] is a special case of our analysis.

VI. PDP Analysis of Mono EH Links

In this section, for both slow and fast fading channels, we consider the PDP analysis of both mono-T and mono-R EH links, with both ARQ and HARQ-CC protocols.

First, we consider the mono-T case. Similar to the analysis of dual EH links, the evolution of the system within a frame can be modeled as a DTMC whose state is represented by the tuple (B_n^t, U_n), where B_n^t and $U_n \in \{-1, 1, \ldots, K\}$ are as defined in Sec. III. Hence, the PDP is given as

$$P_{\mathrm{D}}(K) = \sum_{i=0}^{B_{\max}^t} \pi(i) P_{\mathrm{D}}(K|i, \ell = 1), \tag{27}$$

where $\pi(i)$ denotes the stationary probability that the transmitting EHN has iE_s energy in the battery at the beginning of the frame, and $P_{\mathrm{D}}(K|i, \ell = 1)$ denotes the conditional PDP. In the above, the stationary probabilities can be obtained by using (7). Here, the $(i, j)^{\text{th}}$ entry of the TPM $\boldsymbol{G}'$ equals $\Pr(B_{(M+1)K} = j | B_{MK} = i)$, i.e., it contains the K-step transition probabilities of the battery state. These probabilities can be calculated using the one-step TPM $\boldsymbol{G}_m$, which can in turn be obtained from the TPM for dual EH links defined in (32), by setting $B_{\max}^r = \infty$ and $j_1 = j_2 = \infty$. The expression for $\boldsymbol{G}_m$ is provided in Appendix C.

The conditional PDP, $P_{\mathrm{D}}(K|i, \ell = 1)$, is written as

$$P_{\mathrm{D}}(K|i, \ell = 1) = \sum_{m_t=0}^{K} \binom{K}{m_t} \rho_t^{m_t} (1 - \rho_t)^{K - m_t} p_{\mathrm{D}}(i, m_t). \tag{28}$$

The above equation is obtained using (10) with $m_r = K$ and $\rho_r = 1$. In (28), $p_{\mathrm{D}}(i, m_t)$ denotes the PDP when the transmitter has i units of energy at the beginning of the frame and harvests energy in exactly m_t slots. For both slow and fast fading channels, the $p_{\mathrm{D}}(i, m_t)$ can be obtained from $p_{\mathrm{D}}(i, j, m_t, m_r)$ by setting $j = \infty$, i.e., $\Psi_1 = \kappa_t$ given by (13).

The analysis for mono-T links with HARQ-CC, as well as for mono-R links with ARQ and HARQ-CC can be obtained in a similar fashion. The results are summarized in Table I.

The conditions for operating in the EUR can be obtained using the results of dual EH links, by simply dropping the constraint corresponding to the non-EH node. Similarly, the expressions for the PDP of mono EH links with battery-less EH nodes can be obtained by setting $\rho_t = 1$ or $\rho_r = 1$, corresponding to the node that is connected to the mains.

The results presented thus far correspond to the case where the harvesting processes at the transmitter and receiver are spatially and temporally independent. In the next section, we briefly discuss the extension to the case where the EH processes are correlated.

VII. Extension to Spatially and Temporally Correlated EH Processes

In the subsection below, we show the extension of the PDP analysis to the case where the EH process is temporally correlated, by modeling the process using a stationary Markov model.

TABLE I
Conditional PDP of Mono EH Links

Expression for conditional PDP of mono-T links employing HARQ-CC	
$P_{\mathrm{D}}(K\|i, \ell = 1)$	$\sum_{m_t=0}^{K} \binom{K}{m_t} \rho_t^{m_t} (1 - \rho_t)^{K - m_t} p_{\mathrm{D}}(i, m_t)$
$p_{\mathrm{D}}(i, m_t)$	Obtained using (17) and (19) with $\Psi_1 = \kappa_t$.
Expression for conditional PDP of mono-R links employing ARQ	
$P_{\mathrm{D}}(K\|j, \ell = 1)$	$\sum_{m_r=0}^{K} \binom{K}{m_r} \rho_r^{m_r} (1 - \rho_r)^{K - m_r} p_{\mathrm{D}}(j, m_r)$
$p_{\mathrm{D}}(j, m_r)$	Obtained using Lemma 3 and (15) with $\Psi_1 = \kappa_r$.
Expression for conditional PDP of mono-R links employing HARQ-CC	
$P_{\mathrm{D}}(K\|j, \ell = 1)$	$\sum_{m_r=0}^{K} \binom{K}{m_r} \rho_r^{m_r} (1 - \rho_r)^{K - m_r} p_{\mathrm{D}}(j, m_r)$
$p_{\mathrm{D}}(j, m_r)$	Obtained using (17) and (19) with $\Psi_1 = \kappa_r$.

A. PDP Analysis With a Stationary Markov Energy Harvesting Process

In this subsection, we model the temporal correlation in the EH process using a first order stationary Markov model, which is described by the set of harvesting energy levels, $\mathcal{E} \triangleq \{e_1^t, \ldots, e_{\max}^t\}$, and the probabilities, $p_{a,b} = \Pr\left[E_{n+1}^t = e_b^t | E_n^t = e_a^t\right]$, that e_b^t units of energy is harvested in the $(n+1)^{\text{th}}$ slot, given that e_a^t units of energy was harvested in the n^{th} slot, where both e_a^t and $e_b^t \in \mathcal{E}$. The EH process at the receiver is modeled similarly.

When the EH processes follow a stationary Markov model, the system evolution over a frame depends not only on the initial battery states at the transmitter and receiver, but also on the initial state of the EH Markov chains. Hence, the evolution of the system can be modeled as a DTMC with state denoted by a tuple $(B_n^t, B_n^r, E_n^t, E_n^r, U_n)$. The PDP is given as

$$P_{\mathrm{D}}(K) = \sum_{(i, j, e_a^t, e_c^r)} \pi(i, j, e_a^t, e_c^r) P_{\mathrm{D}}(K|i, j, e_a^t, e_c^r, \ell = 1), \tag{29}$$

where $\pi(i, j, e_a^t, e_c^r)$ denotes the stationary probability that, at the beginning of the frame, the state of the battery and EH process at the transmitter and receiver are (i, j) and (e_a^t, e_c^r), respectively, while $P_{\mathrm{D}}(K|i, j, e_a^t, e_c^r, \ell = 1)$ denotes the PDP conditioned on the state at the beginning of the frame. To obtain the stationary probabilities, using (7), one needs to determine the transition probabilities, $\Pr\left[(i_2, j_2, e_b^t, e_d^r) \mid (i_1, j_1, e_a^t, e_c^r)\right]$, which can be obtained as a straightforward extension of the transition probabilities

given by (32) in Appendix A for the Bernoulli harvesting model. The conditional PDP, $P_{\rm D}(K|i,j,e_a^t,e_c^r,\ell=1)$, can be written as

$$P_{\rm D}(K|i,j,e_a^t,e_c^r,\ell=1)=\sum_{E_t=0}^{Ke_{\max}^t}\sum_{E_r=0}^{Ke_{\max}^r}p(E_t,E_r|e_a^t,e_c^r)\times p_{\rm D}(i,j,E_t,E_r), \quad (30)$$

where $p(E_t,E_r|e_a^t,e_c^r)$ denotes the probability that, during the frame, the transmitter and receiver harvest E_t and E_r units of energy, respectively, given the harvested energy at the beginning of the frame are e_a^t and e_c^r, respectively, and $p_{\rm D}(i,j,E_t,E_r)$ denotes the PDP when the transmitter and receiver batteries have i and j units of energy, respectively, at the beginning of the frame. The $p(E_t,E_r|e_a^t,e_c^r)$ can be calculated using the transition probabilities, $p_{a,b}$, of the stationary Markov model. To compute $p_{\rm D}(i,j,E_t,E_r)$, we use $E_{\rm avl}^t\approx\{i+E_t,B_{\max}^t\}$ and $E_{\rm avl}^r\approx\{j+E_r,B_{\max}^r\}$ and calculate Ψ_1 using Lemma 4. The obtained Ψ_1 can be used to compute $p_{\rm D}(i,j,E_t,E_r)$ using the expression for $p_{\rm D}(i,j,m_t,m_r)$ provided in Sec. IV.

Next, we extend our PDP analysis to the case of spatially correlated EH processes.

B. Extension to Spatially Correlated EH Processes

In case the independence between the EH process of the transmitter and receiver does not hold, the joint distribution of two correlated Bernoulli harvesting processes can be modeled as

$$p(e_t,e_r)=p_{00}(1-e_t)(1-e_r)+p_{01}(1-e_t)e_r+p_{10}e_t(1-e_r)+p_{11}e_te_r, \quad (31)$$

where $e_t,e_r\in\{0,1\}$ are random variables taking nonzero value if energy is harvested at the transmitter and receiver, respectively, and p_{00}, p_{01}, p_{10}, and p_{11} are probability values that add up to 1. To obtain the exact conditional PDP and the 1-step TPM for spatially correlated EH processes, one needs to modify (9) and (32) in Appendix A by replacing $\rho_t\rho_r$ by p_{11}, $\rho_t(1-\rho_r)$ by p_{10} and so on. Also, the above correlated harvesting model reduces to the independent harvesting case when $p_{00}=(1-\rho_t)(1-\rho_r)$, $p_{11}=\rho_t\rho_r$, $p_{10}=\rho_t(1-\rho_r)$ and $p_{01}=(1-\rho_t)\rho_r$.

Further, to obtain the closed-form expressions for the conditional PDP when the harvesting processes at the transmitter and receiver are spatially correlated, we modify (10) as

$$P_{\rm D}(K|i,j,\ell=1)=\sum_{m_t=0}^{K}\sum_{m_r=0}^{K}p'(m_t,m_r)p_{\rm D}(i,j,m_t,m_r),$$

where

$$p'(m_t,m_r)=\sum_{z=\xi_1}^{\xi_2}\binom{K}{z}\frac{(K-z)!}{(m_r-z)!(K-m_t-m_r+z)!}\times\frac{1}{(m_t-z)!}p_{11}^z p_{10}^{(m_t-z)}p_{01}^{(m_r-z)}p_{00}^{(K-m_t-m_r+z)}$$

denotes the probability that the transmitter and receiver harvest energy in exactly m_t and m_r slots, respectively. Here, $\xi_1=\max\{0,m_t+m_r-K\}$ and $\xi_2=\min\{m_t,m_r\}$.

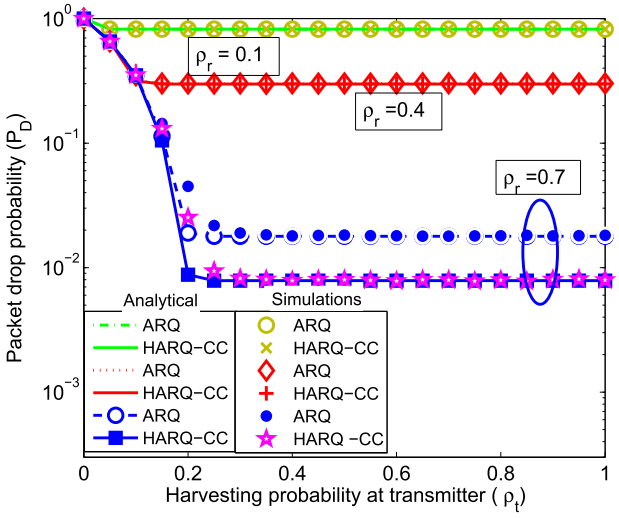

Fig. 5. Dual EH links with slow fading channels: validation of analytical expressions against simulation results. The transmission policy used is [0.5 1.5 2.5 3.5]. The other parameters are $E_s=12$ dB, $\gamma_0=10$ dB, $K=4$, $R=2$ and $B_{\max}^t=B_{\max}^r=20E_s$.

In the next section, we present simulation results to validate the accuracy of the analytical expressions, and illustrate the various cost-performance tradeoffs involved.

VIII. Numerical Results

A. Simulation Setup

We consider a system with slot duration $T_p=100$ ms and carrier frequency 950 MHz. The distance between transmitter and receiver is $d=10d_0$, where $d_0=10$ m is the reference distance and the path loss exponent is $\eta=4$. The additive noise corresponds to a bandwidth of 5 MHz and $T=300$ K. For this system, $E_s=5$ dB corresponds to 100 μJ. To simulate meaningful PDP values (10^{-2} to 10^{-4}), for slow fading channels we choose $E_s=12$ dB and $\gamma_0=10$ dB, while for fast fading channels we set $E_s=5$ dB and $\gamma_0=12$ dB. The channel from the transmitter to the receiver is assumed to be i.i.d. Rayleigh block fading with block length equal to the packet duration and frame duration for the fast and slow fading cases, respectively. The PDP is computed by simulating the transmission of 10^7 packets.

B. Results

1) Performance of Dual EH Links: Figures 5 and 6 present the PDP as a function of ρ_t, in the slow and fast fading cases, respectively. In both the cases, it can be observed that the analytical expressions and simulation results match perfectly. The PDP is dominated by the node which supports the least number of attempts, which, in turn, is determined by the power control policy and EH profiles of the transmitter and receiver.

It can be observed that, for larger values of ρ_r, i.e., for $\rho_r=0.7$ in Fig. 5 and $\rho_r=1$ in Fig. 6, the PDP decreases initially and then it remains unchanged with the increase in ρ_t (e.g., $\rho_t>0.2$ in Fig. 5). This happens because at lower values of ρ_t, the packet drops are dominated by the energy outage at the transmitter which gets mitigated

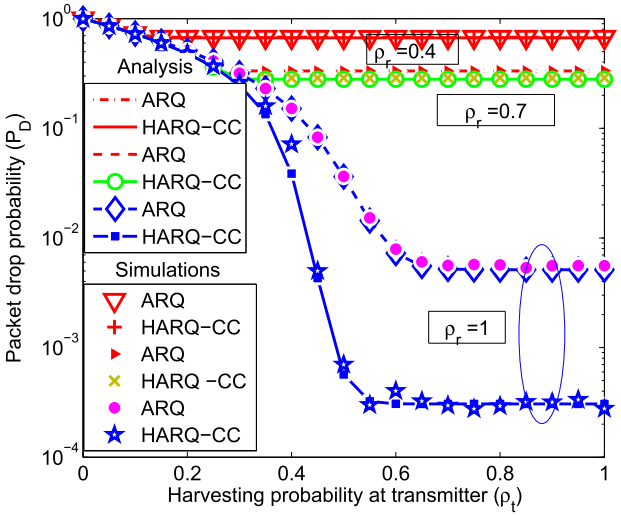

Fig. 6. Dual EH links with fast fading channels: validation of analytical expressions against simulation results. The transmission policy used is [0.5 1.5 2.5 3.5]. The other parameters are $E_s = 5$ dB, $\gamma_0 = 12$ dB, $K = 4$, $R = 2$ and $B^t_{\max} = B^r_{\max} = 20E_s$.

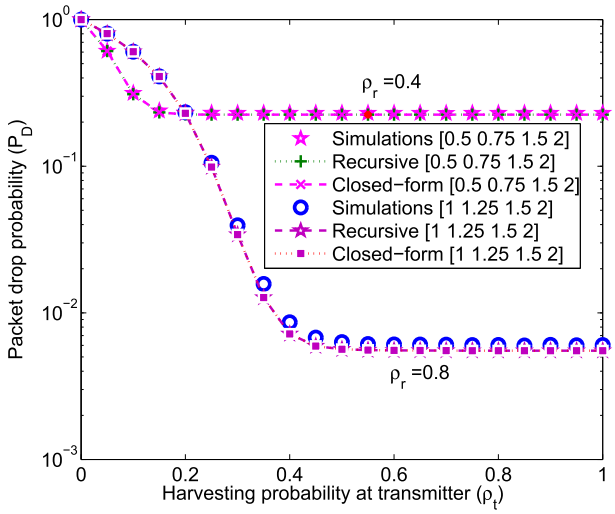

Fig. 7. Accuracy of analytical expressions for small battery regime. The comparison is done for ARQ-based dual EH links over slow fading channels. The size of the batteries at the transmitter and receiver is $B^t_{\max} = B^r_{\max} = 3.5E_s$. Other parameters chosen are $K = 4$, $E_s = 12$ dB, $\gamma_0 = 1$ dB, and $R = 2$.

as ρ_t increases. For higher values of ρ_t and ρ_r, since both nodes harvest enough energy to make all K attempts, packets are dropped only due to the receiver noise or fading, and not due to lack of energy availability. Moreover, in both Figs. 5 and 6, we observe that for lower values of ρ_r (e.g., $\rho_r = 0.4$) and for large enough ρ_t, the randomness of the EH process at the transmitter does not affect the PDP. These regions can be considered to be *partial EUR*, where only one node is able to operate in the EUR. However, the harvesting probability at which an EHN attains the EUR also depends on the power control policy and the EH profile of the other EHN. For example, as shown in both Figs. 5 and 6, the value of ρ_t at which the transmitter achieves the partial EUR increases with the increase in ρ_r.

In Fig. 6, we can observe that, in contrast to the slow fading case, we obtain lower PDP values in the EUR, due to the time-diversity offered by the fast fading channels. Thus, the time-diversity offered by fast fading channels can compensate for lower harvested energy values.

For $\rho_r = 0.7$ and $\rho_r = 1$ in Figs. 5 and 6, respectively, the HARQ-CC outperforms ARQ by approximately a factor of 2 and 10 in the slow and fast fading cases, respectively, in the EUR. However, in both cases, for lower ρ_r, the HARQ-CC does not offer as significant a gain as for $\rho_r = 0.7$ in Fig. 5, and for $\rho_r = 1$ in Fig. 6. This is due to the fact that at lower values of ρ_r, the receiver does not have sufficient energy to exploit the benefits of chase combining. Note that, Figs. 5 and 6 correspond to the scenario when the hypothesis (i) in Lemma 5 is satisfied.

In Fig. 7, we consider a small battery regime to compare the PDP computed using the closed-form analytical expressions against the simulated PDP. We also plot the PDP computed using the *recursive* expression provided in Lemma 1. In this case, we consider two policies: [1 1.25 1.5 2] and [0.5 0.75 1.5 2]. The policies represent two scenarios: in the first case, the policy consumes more than E_s energy in each slot, while, in the latter case, the size of the battery at both transmitter and receiver is not sufficient to store the total energy required by the policy to make all K attempts during a frame. Therefore, in the first case, the hypothesis (ii) of Lemma 5 is satisfied, while in the latter case *neither* of the two hypotheses in Lemma 5 is satisfied. In both these cases, we observe that the simulated results closely match the closed-form analytical expression. For the policy [0.5 0.75 1.5 2], the near-exact match between closed-form PDP and simulated PDP is due to the small impact of the approximation error, as the number of feasible attempts are determined by the energy availability at the receiver in this case. Specifically, for $\rho_t = 1$, the actual number of feasible attempts for the transmitter and receiver are four and three, respectively, while using the approximation in Lemma 5, the estimated number of attempts are three for both the EHNs. However, since the number of feasible attempts under coordinated sleep-wake protocol are determined by the node which can support fewer attempts among the two EHNs, the approximation error does not impact the accuracy of the closed-form PDP.

2) Special Cases (Mono and Zero Energy Buffer EH Links): The results in Fig. 8 demonstrate the PDP of mono-R links. As can be observed from Fig. 8, the value of ρ_r at which the receiver attains EUR increases with R, because of the higher average energy consumption. Fig. 9 contains the results for dual EH links with zero energy buffers. Again, the analytical expressions and simulation results match perfectly. Also, the results in Figs. 8 and 9 again highlight the fact that the use of HARQ-CC results in better performance. For Dual EH links, even without an energy buffer, at higher values of ρ_r, the use of HARQ-CC results in performance improvement over ARQ approximately by a factor of 2. However, for mono-R links, the gains occur only after the receiver harvests enough energy to enter the EUR.

3) Comparison of RIPs With SoC Aware Optimal Policies: In Fig. 10, we compare the performance of a judiciously chosen RIP with the optimal SoC-aware policy,

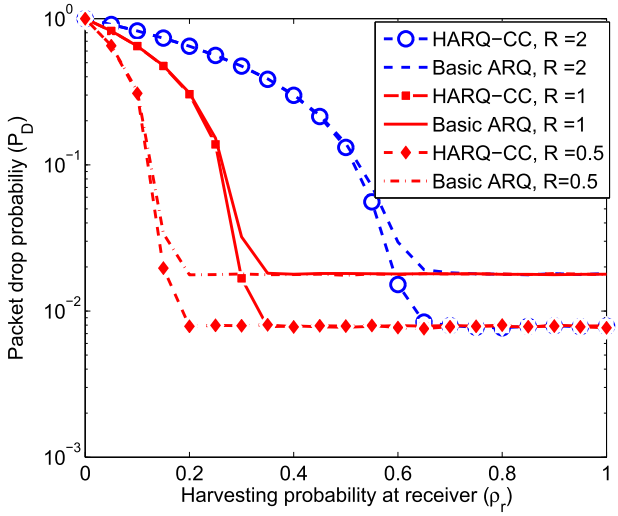

Fig. 8. PDP of mono-R links with a slow fading channel. The transmission policy used is [0.5 1.5 2.5 3.5]. The other parameters are $E_s = 10$ dB, $\gamma_0 = 12$ dB, $K = 4$, and $B^r_{\max} = 20E_s$.

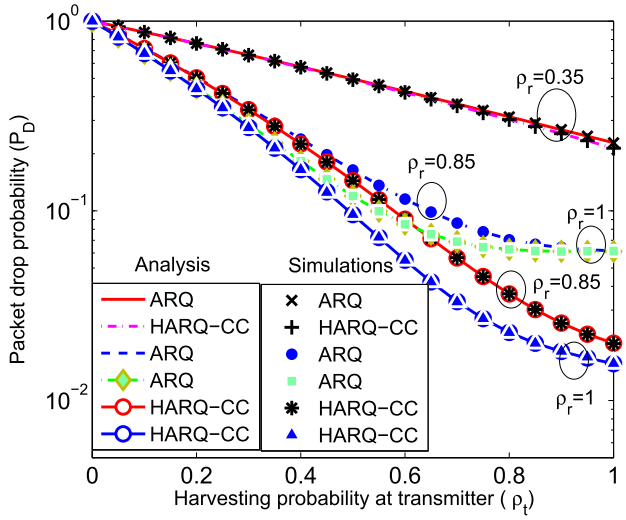

Fig. 9. Dual EH links with zero energy buffer nodes: validation of analytical expressions against simulations. The other parameters are $E_s = 12$ dB, $\gamma_0 = 10$ dB, $K = 4$, and a slow fading channel.

for mono-T EH links. The optimal SoC-aware policy is designed using the MDP [17]. The performance is compared for both slow and fast fading channels with different number of quantization levels for the channel. As seen in Fig. 10, a judiciously chosen RIP outperforms the MDP based policies. While the MDP approach should provide the optimal policy in theory, practically computing the optimal policy is difficult as one needs to quantize the channel and battery for the MDP formulation to be applicable, and a fine quantization makes it numerically difficult to evaluate the optimal policy. Hence, in practice, we see that a well-designed RIP can even outperform the SoC-aware MDP based policy.

IX. Conclusions

In this paper, we presented a general framework to analyze the PDP of dual EH links with retransmissions. We considered SoC-unaware policies, and slow and fast fading channels.

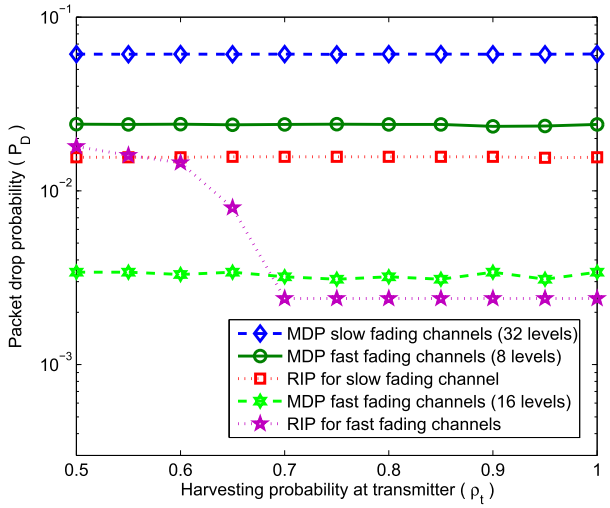

Fig. 10. Performance comparison of RIPs for ARQ based mono-T links: performance of RIPs compared with the optimal policies designed using an MDP that has access to the SoC information [17]. For $\rho_t \geq 0.7$, the RIP outperforms the MDP based policy. Number of transmissions and energy buffer size are $K = 4$ and $B^t_{\max} = 40E_s$, respectively. Also, the maximum energy used per attempt $L_{\max} = 2E_s$, $E_s = 5$ dB and target SNR $\gamma_0 = 12$ dB for the fast fading channel, and $L_{\max} = 4E_s$, $E_s = 12$ dB and target SNR $\gamma_0 = 10$ dB for the slow fading channel.

We obtained closed form expressions for the PDP with both ARQ and HARQ-CC, by modeling the system evolution as a discrete-time Markov chain. We extended the analysis to handle correlated harvesting processes at the transmitter and receiver. The PDP expressions for mono EH links are obtained as a special case of the analysis of dual EH links. Our analysis is useful in quantifying the impact of various system parameters such as the energy harvesting profiles, and energy buffer sizes of both transmitter and receiver, channel coherence time, transmit and receive power control policies etc., on the PDP. We also characterized the energy unconstrained regime of dual EH links and obtained simplified expressions for the PDP in the special cases of zero and infinite size energy buffers. Our future work uses the closed form expressions derived in this paper to find optimal RIPs for dual as well as mono EH links. Further extensions of this work could consider leveraging the temporal correlation of the fading channel based on the implicit channel state feedback available through ACK/NACK messages.

Appendix

A. Transition Probability Matrix, $\mathbf{G}$, for Dual EH Links

The probability of transition from state (i_1, j_1, ℓ_1) to (i_2, j_2, ℓ_2) is $G^{i_2,j_2,\ell_2}_{i_1,j_1,\ell_1} = \Pr\left(B^t_{n+1} = i_2, B^r_{n+1} = j_2, U_{n+1} = \ell_2 \middle| B^t_n = i_1, B^r_n = j_1, U_n = \ell_1\right)$, where $i_1, i_2, j_1, j_2 \in \{0, 1, \ldots, \infty\}$, and $\ell_1, \ell_2 \in \{-1, 1, \ldots, K\}$. For $\ell_1 \in \{1, \ldots, K\}$, $i_1 \geq L_{\ell_1}$ and $j_1 \geq R$, the $G^{i_2,j_2,\ell_2}_{i_1,j_1,\ell_1}$ is written as given in (32), as shown at the top of the next page.

In (32), $\Pr[\gamma_n < \gamma_0]$ for both slow and fast fading channels and ARQ is given by (2), while for HARQ-CC with slow and fast fading channels it is obtained using $\Psi_1 = \ell_1$ in (17) and (19), respectively. The terms in the above transition probability expression are obtained by considering the events

$$G_{i_1,j_1,\ell_1}^{i_2,j_2,\ell_2} = \begin{cases} \rho_t\rho_r \Pr\left[\gamma_n < \gamma_0\right], & i_2 = i_1 - L_{\ell_1} + 1, \quad j_2 = j_1 - R + 1, \quad \ell_2 = \ell_1 + 1, \\ \rho_t\rho_r \Pr\left[\gamma_n \geq \gamma_0\right], & i_2 = i_1 - L_{\ell_1} + 1, \quad j_2 = j_1 - R + 1, \quad \ell_2 = -1, \\ (1-\rho_t)\rho_r \Pr\left[\gamma_n < \gamma_0\right], & i_2 = i_1 - L_{\ell_1}, \quad j_2 = j_1 - R + 1, \quad \ell_2 = \ell_1 + 1, \\ (1-\rho_t)\rho_r \Pr\left[\gamma_n \geq \gamma_0\right], & i_2 = i_1 - L_{\ell_1}, \quad j_2 = j_1 - R + 1, \quad \ell_2 = -1, \\ \rho_t(1-\rho_r) \Pr\left[\gamma_n < \gamma_0\right], & i_2 = i_1 - L_{\ell_1} + 1, \quad j_2 = j_1 - R, \quad \ell_2 = \ell_1 + 1, \\ \rho_t(1-\rho_r) \Pr\left[\gamma_n \geq \gamma_0\right], & i_2 = i_1 - L_{\ell_1} + 1, \quad j_2 = j_1 - R, \quad \ell_2 = -1, \\ (1-\rho_t)(1-\rho_r) \Pr\left[\gamma_n < \gamma_0\right], & i_2 = i_1 - L_{\ell_1}, \quad j_2 = j_1 - R, \quad \ell_2 = \ell_1 + 1, \\ (1-\rho_t)(1-\rho_r) \Pr\left[\gamma_n \geq \gamma_0\right], & i_2 = i_1 - L_{\ell_1}, \quad j_2 = j_1 - R, \quad \ell_2 = -1, \\ 0, & \text{otherwise.} \end{cases} \tag{32}$$

that need to occur for the particular transition to happen. For example, the transition in the first case happens if both transmitter and receiver harvest the energy in the current slot, and a decoding failure occurs in the current attempt. Note that, in (32), for simplicity, the transition probabilities are written for infinite buffer size at both transmitter and receiver. However, as shown in Appendix C for the mono EH case, the expression can be easily modified for the finite capacity battery case. The transition probabilities for the other cases, e.g., $i_1 \leq L_{\ell_1}$ and $j_1 \geq R$, are obtained similarly, and details are provided in [44].

B. Proof of Lemma 4

During a frame, the transmitter has at most $i + m_t$ units of energy for its use. If $i + m_t \leq B_{\max}^t$, then $E_{\text{avl}}^t = i + m_t$, while if $i + m_t > B_{\max}^t$, then $E_{\text{avl}}^t \leq i + m_t$, i.e., the EHN may not be able to use the entire energy, $i + m_t$, depending on the order in which energy arrivals and departures occur. Furthermore, for the case when $i + m_t > B_{\max}^t$, $E_{\text{avl}}^t = B_{\max}^t + \xi$ where $0 \leq \xi \leq K$ is a random variable which is equal to the number of slots where energy is harvested *and* $B_n^t < B_{\max}^t$. For $i + m_t > B_{\max}^t$, we approximate the available energy as $E_{\text{avl}}^t \approx B_{\max}^t$, and ignore ξ. For policies such that $\sum_{\ell=1}^K L_\ell \leq B_{\max}^t$, ignoring ξ for $i + m_t > B_{\max}^t$ will also result in K feasible attempts. Using a similar argument, we can approximate E_{avl}^r. Hence, when $\sum_{\ell=1}^K L_\ell \leq B_{\max}^t$ and $KR \leq B_{\max}^r$, the available energy can be well approximated as $E_{\text{avl}}^t \approx \min\{i + m_t, B_{\max}^t\}$ and $E_{\text{avl}}^r \approx \min\{j + m_r, B_{\max}^r\}$.

The proof of statement (ii) in the Lemma follows from the observation that a node that employs a policy that uses more than one unit of energy in each attempt (i.e., $L_\ell \geq 1$ for all $1 \leq \ell \leq K$) always has the space to accommodate one unit of energy. Hence, if the transmitter harvests energy in m_t slots and has i units of energy in the battery at the beginning of the frame, then the total available energy at the transmitter is given by $E_{\text{avl}}^t = i + m_t$. Similarly, $E_{\text{avl}}^r = j + m_r$ when $R \geq 1$.

C. Transition Probability Matrix $\boldsymbol{G}_m$ for Mono EH Links

For mono-T EH links, the probability of transition from state (i, ℓ_1) to (j, ℓ_2) is $G_{(m)i,\ell_1}^{j,\ell_2} = \Pr(B_n = j, U_{n+1} = \ell_2 | B_n = i, U_n = \ell_1)$, where $i, j \in \{0, 1, \ldots, B_{\max}^t\}$ and $\ell_1, \ell_2 \in \{-1, 1, \ldots, K\}$. For $\ell_1 \in \{1, \ldots, K\}$ and $i \geq L_{\ell_1}$

$$G_{(m)i,\ell_1}^{j,\ell_2} = \begin{cases} \rho_t \Pr\left[\gamma_n < \gamma_0\right], & j = \min\left\{i - L_{\ell_1} + 1, B_{\max}^t\right\}, \\ & \ell_2 = \ell_1 + 1, \\ \rho_t \Pr\left[\gamma_n \geq \gamma_0\right], & j = \min\{i - L_{\ell_1} + 1, B_{\max}^t\}, \\ & \ell_2 = -1, \\ (1-\rho_t) \Pr\left[\gamma_n < \gamma_0\right], & j = i - L_{\ell_1}, \quad \ell_2 = \ell_1 + 1, \\ (1-\rho_t) \Pr\left[\gamma_n > \gamma_0\right], & j = i - L_{\ell_1}, \quad \ell_2 = -1, \\ 0, & \text{otherwise.} \end{cases}$$

In the above, $\Pr[\gamma_n < \gamma_0]$ for ARQ is written using (2), while for HARQ-CC with slow and fast fading channels, it can be computed using (17) and (19), respectively, with $\Psi_1 = \ell_1$.

REFERENCES

[1] M. K. Sharma and C. R. Murthy, "Packet drop probability analysis of ARQ and HARQ-CC with energy harvesting transmitters and receivers," in *Proc. IEEE GlobalSIP*, Dec. 2014, pp. 148–152.

[2] C. Yuen, M. Elkashlan, Y. Qian, T. Q. Duong, L. Shu, and F. Schmidt, "Energy harvesting communications: Part 1 [Guest Editorial]," *IEEE Commun. Mag.*, vol. 53, no. 4, pp. 68–69, Apr. 2015.

[3] S. Kim, R. Fonseca, and D. Culler, "Reliable transfer on wireless sensor networks," in *Proc. 1st Annu. IEEE Commun. Soc. Sensor Ad Hoc Commun. Netw. (SECON)*, Oct. 2004, pp. 449–459.

[4] *IEEE Standard for Local and Metropolitan Area Networks—Part 15.4: Low-Rate Wireless Personal Area Networks (LR-WPANs)*, IEEE Standard 802.15.4-2011 (Revision of IEEE Standard 802.15.4-2006), Sep. 2011, pp. 1–314.

[5] T. V. K. Chaitanya and E. G. Larsson, "Optimal power allocation for hybrid ARQ with chase combining in i.i.d. rayleigh fading channels," *IEEE Trans. Commun.*, vol. 61, no. 5, pp. 1835–1846, May 2013.

[6] H. Seo and B. G. Lee, "Optimal transmission power for single-and multi-hop links in wireless packet networks with ARQ capability," *IEEE Trans. Commun.*, vol. 55, no. 5, pp. 996–1006, May 2007.

[7] M. K. Sharma and C. R. Murthy, "On design of dual energy harvesting communication links with retransmission," *IEEE Trans. Wireless Commun.*, submitted for publication.

[8] O. Ozel and S. Ulukus, "Achieving AWGN capacity under stochastic energy harvesting," *IEEE Trans. Inf. Theory*, vol. 58, no. 10, pp. 6471–6483, Oct. 2012.

[9] R. Rajesh, V. Sharma, and P. Viswanath, "Capacity of Gaussian channels with energy harvesting and processing cost," *IEEE Trans. Inf. Theory*, vol. 60, no. 5, pp. 2563–2575, May 2014.

[10] D. Shaviv, P.-M. Nguyen, and A. Ozgur. (Jul. 2015). "Capacity of the energy harvesting channel with a finite battery." [Online]. Available: https://arxiv.org/abs/1506.02024

[11] A. Seyedi and B. Sikdar, "Modeling and analysis of energy harvesting nodes in wireless sensor networks," in *Proc. 46th Annu. Allerton Conf. Commun., Control, Comput.*, Sep. 2008, pp. 67–71.

[12] V. Sharma, U. Mukherji, V. Joseph, and S. Gupta, "Optimal energy management policies for energy harvesting sensor nodes," *IEEE Trans. Wireless Commun.*, vol. 9, no. 4, pp. 1326–1336, Apr. 2010.
[13] O. Ozel, K. Tutuncuoglu, J. Yang, S. Ulukus, and A. Yener, "Transmission with energy harvesting nodes in fading wireless channels: Optimal policies," *IEEE J. Sel. Areas Commun.*, vol. 29, no. 8, pp. 1732–1743, Sep. 2011.
[14] C. K. Ho and R. Zhang, "Optimal energy allocation for wireless communications with energy harvesting constraints," *IEEE Trans. Signal Process.*, vol. 60, no. 9, pp. 4808–4818, Sep. 2012.
[15] C. Huang, R. Zhang, and S. Cui, "Optimal power allocation for outage probability minimization in fading channels with energy harvesting constraints," *IEEE Trans. Wireless Commun.*, vol. 13, no. 2, pp. 1074–1087, Feb. 2014.
[16] B. Medepally, N. B. Mehta, and C. R. Murthy, "Implications of energy profile and storage on energy harvesting sensor link performance," in *Proc. IEEE Globecom*, Dec. 2009, pp. 1–6.
[17] A. Aprem, C. R. Murthy, and N. B. Mehta, "Transmit power control policies for energy harvesting sensors with retransmissions," *IEEE J. Sel. Topics Signal Process.*, vol. 7, no. 5, pp. 895–906, Oct. 2013.
[18] A. M. Devraj, M. K. Sharma, and C. R. Murthy, "Power allocation in energy harvesting sensors with ARQ: A convex optimization approach," in *Proc. IEEE GlobalSIP*, Dec. 2014, pp. 208–212.
[19] H. Mahdavi-Doost and R. D. Yates, "Energy harvesting receivers: Finite battery capacity," in *Proc. IEEE Int. Symp. Inf. Theory*, Jul. 2013, pp. 1799–1803.
[20] R. D. Yates and H. Mahdavi-Doost, "Energy harvesting receivers: Packet sampling and decoding policies," *IEEE J. Sel. Areas Commun.*, vol. 33, no. 3, pp. 558–570, Mar. 2015.
[21] S. Ulukus *et al.*, "Energy harvesting wireless communications: A review of recent advances," *IEEE J. Sel. Areas Commun.*, vol. 33, no. 3, pp. 360–381, Mar. 2015.
[22] A. Arafa and S. Ulukus, "Single-user and multiple access channels with energy harvesting transmitters and receivers," in *Proc. IEEE Global Conf. Signal Inf. Process. (GlobalSIP)*, Dec. 2014, pp. 213–217.
[23] S. Zhou, T. Chen, W. Chen, and Z. Niu, "Outage minimization for a fading wireless link with energy harvesting transmitter and receiver," *IEEE J. Sel. Areas Commun.*, vol. 33, no. 3, pp. 496–511, Mar. 2015.
[24] N. Michelusi, L. Badia, R. Carli, L. Corradini, and M. Zorzi, "Energy management policies for harvesting-based wireless sensor devices with battery degradation," *IEEE Trans. Commun.*, vol. 61, no. 12, pp. 4934–4947, Dec. 2013.
[25] D. D. Testa and M. Zorzi, "Optimal policies for two-user energy harvesting device networks with imperfect state-of-charge knowledge," in *Proc. IEEE Inf. Theory Appl. Workshop*, Feb. 2014, pp. 1–5.
[26] N. Michelusi, L. Badia, R. Carli, K. Stamatiou, and M. Zorzi, "Correlated energy generation and imperfect state-of-charge knowledge in energy harvesting devices," in *Proc. 8th IWCMC*, Aug. 2012, pp. 401–406.
[27] N. Michelusi, K. Stamatiou, L. Badia, and M. Zorzi, "Operation policies for energy harvesting devices with imperfect state-of-charge knowledge," in *Proc. IEEE ICC*, Jun. 2012, pp. 5782–5787.
[28] R. Srivastava and C. E. Koksal, "Basic performance limits and tradeoffs in energy-harvesting sensor nodes with finite data and energy storage," *IEEE/ACM Trans. Netw.*, vol. 21, no. 4, pp. 1049–1062, Aug. 2013.
[29] T. V. K. Chaitanya and E. G. Larsson, "Outage-optimal power allocation for hybrid ARQ with incremental redundancy," *IEEE Trans. Wireless Commun.*, vol. 10, no. 7, pp. 2069–2074, Jul. 2011.
[30] L. Chen *et al.*, "Range extension of passive wake-up radio systems through energy harvesting," in *Proc. IEEE ICC*, Jun. 2013, pp. 1549–1554.
[31] *Indy RS2000 RFID Reader*, accessed on Sep. 8, 2016. [Online]. Available: http://www.impinj.com/
[32] *TX91501 Powercaster transmitter*, accessed on Sep. 15, 2016. [Online]. Available: http://www.powercastco.com/
[33] J. Lei, R. Yates, and L. Greenstein, "A generic model for optimizing single-hop transmission policy of replenishable sensors," *IEEE Trans. Wireless Commun.*, vol. 8, no. 2, pp. 547–551, Feb. 2009.
[34] C. K. Ho and R. Zhang, "Optimal energy allocation for wireless communications powered by energy harvesters," in *Proc. IEEE Int. Symp. Inf. Theory*, Jun. 2010, pp. 2368–2372.
[35] C. K. Ho, P. D. Khoa, and P. Ming, "Markovian model for harvested energy in wireless communication," in *Proc. IEEE ICCS*, Nov. 2010, pp. 311–315.
[36] S. Wei, W. Guan, and K. J. R. Liu, "Power scheduling for energy harvesting wireless communications with battery capacity constraint," *IEEE Trans. Wireless Commun.*, vol. 14, no. 8, pp. 4640–4653, Aug. 2015.
[37] I. S. Kim, "Nonlinear state of charge estimator for hybrid electric vehicle battery," *IEEE Trans. Power Electron.*, vol. 23, no. 4, pp. 2027–2034, Jul. 2008.
[38] R. Xiong, H. He, F. Sun, and K. Zhao, "Evaluation on state of charge estimation of batteries with adaptive extended Kalman filter by experiment approach," *IEEE Trans. Veh. Technol.*, vol. 62, no. 1, pp. 108–117, Jan. 2013.
[39] M. Coleman, C. K. Lee, C. Zhu, and W. G. Hurley, "State-of-charge determination from EMF voltage estimation: Using impedance, terminal voltage, and current for lead-acid and lithium-ion batteries," *IEEE Trans. Ind. Electron.*, vol. 54, no. 5, pp. 2550–2558, Oct. 2007.
[40] K. Tutuncuoglu and A. Yener, "Communicating with energy harvesting transmitters and receivers," in *Proc. Inf. Theory Appl. Workshop (ITA)*, Feb. 2012, pp. 240–245.
[41] J. Vazifehdan, R. V. Prasad, M. Jacobsson, and I. Niemegeers, "An analytical energy consumption model for packet transfer over wireless links," *IEEE Commun. Lett.*, vol. 16, no. 1, pp. 30–33, Jan. 2012.
[42] I. Krikidis, T. Charalambous, and J. S. Thompson, "Buffer-aided relay selection for cooperative diversity systems without delay constraints," *IEEE Trans. Wireless Commun.*, vol. 11, no. 5, pp. 1957–1967, May 2012.
[43] Y. Zhang *et al*, "A batteryless 19μW MICS/ISM-band energy harvesting body sensor node SoC for ExG applications," *IEEE J. Solid-State Circuits*, vol. 48, no. 1, pp. 199–213, Jan. 2013.
[44] M. K. Sharma and C. R. Murthy, "Transition probabilities for DTMC modeling of dual and mono energy harvesting links," Indian Inst. Sci., Bangalore, India, Tech. Rep. [Online]. Available: http://www.ece.iisc.ernet.in/~cmurthy/SPCLab/lib/exe/fetch.php?media=dualehdetails.pdf

Mohit K. Sharma received the B.E. degree in electronics and communication engineering from the University of Rajasthan, Jaipur, India, in 2006, and the M.Tech. degree in signal processing from the IIT Guwahati, Guwahati, India, in 2010. He is currently pursuing the Ph.D. degree in electrical communication engineering with the Indian Institute of Science, Bangalore, India. His research interests are primarily in the area of energy harvesting and resource allocation for wireless communications.

Chandra R. Murthy (S'03–M'06–SM'11) received the B.Tech. degree in electrical engineering from the IIT Madras, Chennai, in 1998, the M.S. degree in electrical and computer engineering from Purdue University, in 2000, and the Ph.D. degree in electrical and computer engineering from the University of California, San Diego, CA, USA, in 2006. From 2000 to 2002, he was an Engineer with Qualcomm Inc., where he was involved in WCDMA baseband transceiver design and 802.11b baseband receivers. From 2006 to 2007, he was a Staff Engineer with Beceem Communications Inc., where he was involved in advanced receiver architectures for the 802.16e Mobile WiMAX standard. In 2007, he joined the Department of Electrical Communication Engineering, Indian Institute of Science, Bangalore, India, where he is currently an Associate Professor.

His research interests are in the areas of energy harvesting communications, multiuser MIMO systems, and sparse signal recovery techniques applied to wireless communications. He was an Associate Editor of the IEEE SIGNAL PROCESSING LETTERS from 2012 to 2016. He is an elected member of the IEEE SPCOM Technical Committee from 2014 to 2016. He is currently serving as the Chair of the IEEE Signal Processing Society, Bangalore Chapter, and an Associate Editor of the IEEE TRANSACTIONS ON SIGNAL PROCESSING. He received the best paper award in communications at the National Conference on Communications in 2014.